RESEARCH ARTICLE

Dynamic skin signatures of cuttlefish internal states

Sophie Cohen-Bodénès[1] and Peter Neri[1]

ABSTRACT

Cuttlefish skin is a powerful rendering device, capable of producing extraordinary changes in visual appearance over a broad range of temporal scales. This unique ability is typically associated with camouflage, however cuttlefish often produce skin patterns that do not appear connected with the surrounding environment, such as fast large-scale fluctuations with wave-like characteristics. Little is known about the functional significance of these dynamic patterns. In this study, we manipulate the internal state of cuttlefish without altering their sensory environments, and study potential changes in the associated pattern dynamics. When cuttlefish are engaged in feeding, we observe accentuated dynamics of specific pattern components within the theta frequency range, with additional evidence of increased display for other components. These changes disappear during the post-feeding phase, which resembles the pre-feeding phase, indicating that they last for a relatively short time between 10 and 20 minutes. Our findings therefore reveal specific alterations of skin pattern dynamics that correspond to changes of internal state associated with self-driven non-sensory behavior.

KEYWORDS: cuttlefish cognition, spectral profile, theta oscillations, principal component analysis, machine learning

INTRODUCTION

The cryptic abilities of cuttlefish, known as "chameleons of the sea," are justly celebrated as stunning examples of animal camouflage. Cuttlefish can achieve nearly complete perceptual disappearance against their natural environment (Kelman et al., 2008), and their skin repertoire is able to approximate specific features of artificial backgrounds (Barbosa et al., 2008; Chiao et al., 2010; Osorio et al., 2022). They also engage in complex mimicry, for example by impersonating crabs to the extent of incorporating characteristic locomotory behaviors (Okamoto et al., 2017). To achieve such degree of fidelity in reproducing the surrounding environment, they must rely not only on powerful mechanisms for changing their own appearance, but also on sophisticated visual processes for acquiring information about the appearance of the environment in the first place (Kelman et al., 2008; Reiter and Laurent, 2020). Little is known about the physiology of the cuttlefish visual system, however there is now sufficient behavioral evidence to conclude that they have access to most visual cues commonly studied in other animals, like motion (Zylinski et al., 2009) and stereoscopic depth (Feord et al., 2020; El Nagar et al., 2021).

Skin patterning is not restricted to camouflage, however. Observational studies of cuttlefish and other cephalopods have identified dynamic patterns that are associated with specific interactions between conspecifics, such as the chromatic pulse pattern displayed by rival male cuttlefish engaged in aggressive or territorial behavior (How et al., 2017), or the passing wave pattern displayed during hunting (Hanlon and Messenger, 1996). Most of our knowledge about cuttlefish communication through skin signalling comes from anecdotal examination of video-recorded examples (How et al., 2017), rather than quantitative measurements under controlled conditions. For this reason, it is possible that the function tentatively ascribed to specific dynamic patterns may not correspond to its actual significance for the animal. Notwithstanding this limitation, it is clear that skin patterning does play a role in some forms of communication that bear no obvious connection with camouflage (Langridge et al., 2007; Galán et al., 2020).

In addition to the two functions outlined above, namely camouflage and communication, there is a third potential behavior that may be connected with skin patterning: the adoption of specific internal states. For example, it is conceivable that mood may be reflected by certain skin patterns, or other internal states like fear (Boyer and Swierk, 2017; Greenberg, 2002). There is currently no concrete evidence to support this speculation, however informal observation of cuttlefish during natural behavior (How et al., 2017) suggests that it is not far-fetched to imagine that their internal state may be associated with specific skin patterns that carry neither cryptic nor communicative functions (in the sense of direct communication with other animals). Our goal was to explore this hypothesis under conditions that would enable a sufficient degree of experimental control to support quantitative analysis of selective changes in skin patterning induced by changes of internal state.

MATERIALS AND METHODS

Animals and husbandry

We conducted behavioral experiments using 13 adult cuttlefish (Sepia officinalis) ranging in age between 3 months ($\sim$ 3 cm mantle length) and 12 months ($\sim$15 cm mantle length). All animals were reared from eggs and maintained from hatchling following established guidelines (Fiorito et al., 2015), either at our facility in Paris or at the authorized institutional supplier Aquarium de la Rochelle (La Rochelle, France). Eggs were collected from the Atlantic Ocean and cuttlefish were reared in captivity (hatched from eggs) by a team of biologists specialized in cuttlefish breeding. When eggs or juveniles were transported from Aquarium La Rochelle to our facility, transportation was optimized by oxygenation enrichment, noise/vibration minimization in a cool specialized container without light exposure, and following food deprivation before transport to avoid accumulation of toxic ammonia level. Once eggs/juveniles reached our facility, they were acclimatized

[1]Laboratoire des Systèmes Perceptifs, École Normale Supérieure, 29 rue d'Ulm, Paris 75005 (France)

Authors for correspondence: (sophie.bodenes@gmail.com; neri.peter@gmail.com)

Received XXXX; revised XXXX

in three artificial marine water tanks (300 L each) for 2 hours. Their health was closely monitored (every hour) for the subsequent 48 hours, and daily until natural death (we carried out euthanization with a MgCl2 solution whenever necessary). When handling eggs, we introduced additional air pumps to provide sufficient oxygenation for their development.

We ensured that the environment of all three fiberglass tanks approximated the natural habitat as close as possible, while at the same time providing adequate monitoring of water quality and animal health. Tanks operated a closed water system that allowed constant monitoring and optimization of water parameters, and contained various oxygen pumps, skimmer, mechanical/biological filtration, and carbon filters for ink removal. At the same time, we introduced sand enrichment (7-cm layer of natural marine uniform sand with granulometry of 1–4 mm, enriched with natural pebbles of different size/color placed randomly across the tank), natural Atlantic ocean shells, and live rocks (∼15 live rocks of different sizes for a total of ∼20 kg per tank) to provide shelter, and more generally to encourage cuttlefish expression of their full behavioral repertoire (burying in sand, establishing territories and dominance hierarchies, protection from lighting in shadowed areas provided by rocks). Tanks were visually isolated from one another to prevent cuttlefish from interacting with animals in other tanks, and tank surface was opacified to minimize mirror reflections. We allowed a maximum of five animals per tank, limited to one individual whenever the potential for aggressive behavior was observed. We established a light/dark cycle of 12-hour/12-hour, and only conducted experiments during the day. Live food was provided three times a day: at 9 am, at 2 pm, and at 8 pm. We never deprived animals, instead food was systematically provided so that cuttlefish could hunt at will (especially during the night) and would not engage in aggressive behavior for food competition. From hatchling to 1 month of age, cuttlefish were fed a mixture of live Artemias and live Mysis. Once they reached 1 month of age, they were fed bigger live marine shrimps (*Palaemonetes vulgaris*, provided by Camargues Peches, Aquadip) and live crabs (provided by Aquarium de Paris) especially raised for feeding marine animals reared in captivity.

Experimental procedure

Our goal was to record cuttlefish behavior under conditions that would approximate its natural spontaneous state. For this reason, we did not interfere with their daily routine and never moved animals to a different tank for testing. Our observational experiments are therefore classed below threshold for explicit ethics approval as expressed in Directive 63/10. We nevertheless seeked and obtained validation by the veterinary official of our Biology Department (IBENS, École Normale Supérieure). When a cuttlefish settled within a specific area of its choice, we fixed an underwater camera (GoPro Hero7) above the tank to record the mantle for ∼2 hours, three times a day, over a period of ∼9 months. Cuttlefish were used to the presence of the camera and did not appear to express signaling patterns in specific response to camera positioning. Experimenters left the room during recording sessions to avoid signalling patterns specific to their presence.

Video segment classification/selection

Each experimental session produced ∼2 hours of continuous video recording. We extracted segments from the associated video file and classed them into one of the three main conditions (before, during, and after eating). At the start of this procedure, we provisionally defined the following epochs: the epoch 'before' eating started 5 minutes after the beginning of video recording (to exclude initial potential responses to camera placement), and ended right before the introduction of food (live preys) into the tank; the epoch 'during' eating started once the prey was fully inside the buccal mass, and ended when the animal stopped producing buccal movements; the epoch 'after' eating started 5 minutes after the end of the 'during' phase, and continued to the end of the video recording session. After completing this preliminary subdivision of different sections within the movie, we excluded segments from each section according to the following criteria: 1) the animal performed large movements towards other areas of the tank; 2) the animal disappeared from view; 3) the hand of the experimenter was visible, for example during introduction of the prey; 4) live preys were visible around the cuttlefish. In all these instances, segments were excluded to minimize the potential contributions of confounding factors and/or to facilitate subsequent tracking by our algorithm (see below). Following the above procedures, the allocation of data mass to the three main conditions was 42% before, 25% during, and 33% after eating.

Tracking/alignment

We wrote in-house software to identify the position of the animal on every frame, and to align the mantle across frames (see **Supplementary Video**). More specifically, we created labelling software to manually mark the position of the two eyes (indicated by red/green dots in **Figure 1A**) and the tail (rear end of the mantle, aligned with posterior segment of white square in **Figure 1A**) for a small subset (<0.1%) of the frames. We augmented the resulting labelled dataset via rotation/flipping, and trained a modified version of the Mask-RNN algorithm (He et al., 2017) to identify corresponding markers in unlabelled images. The output from this stage was submitted to a regularization algorithm that enforced consistency for labels across frames, such as stable inter-eye distance, correction of label inversion across eyes, and pruning of large sudden displacements. We then extracted from each image a square region with size equal to twice the distance between the two eyes, positioned such that the anterior segment aligned with the two eyes and its middle point matched the middle point between the eyes (see examples in **Figure 1A–F**). We converted the resulting square images to monochrome (average of three color guns), applied left-right symmetry (effectively restricting our analysis to bilateral information), rescaled them to a common size of 32×32 pixels to enforce uniformity across different recording sessions and animal sizes, and aligned them to a common coordinate frame (**Figure 1G–K**). To exclude contributions from elements outside the mantle, we further extracted the central square region of each frame (indicated by blue square outlines in **Figure 1G–K**). This procedure generated a large stack of ∼1.6 million images, each image containing 16×16 pixels. Below we refer to this dataset as the 'main' stack.

Principal component analysis

We applied standard principal component analysis (PCA) with varimax rotation to the main stack obtained from tracking/alignment (detailed above). Prior to PCA, the submitted stack was normalized so that each pixel had zero mean and unit standard deviation across frames. In the 'aggregate' analysis, PCA was applied to the entire main stack without differentiating across

Journal of Experimental Biology (2019) 00, jebxxxxxx. doi:10.1242/jeb.xxxxxx

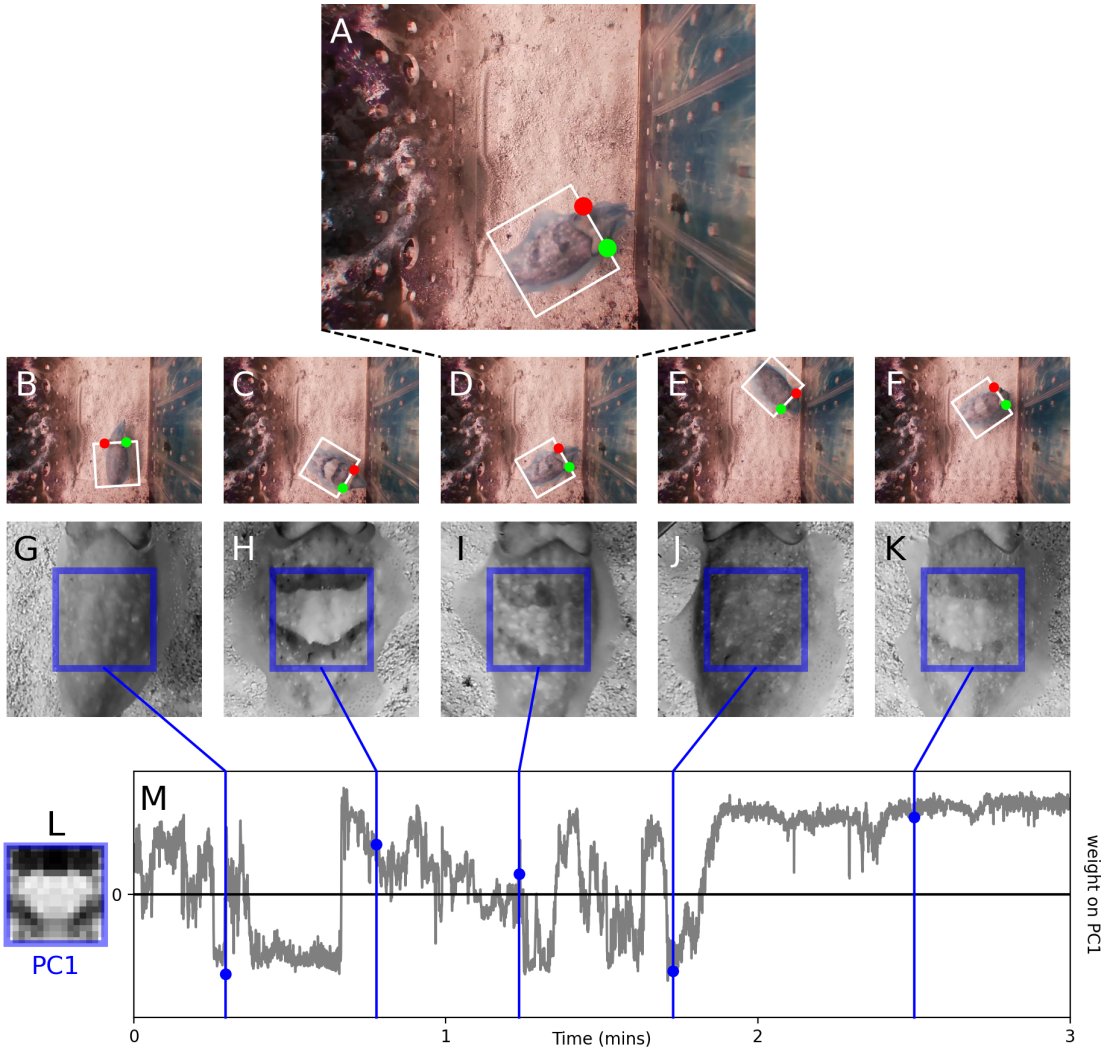

Fig. 1. Cuttlefish were filmed from above without disrupting their daily routine/environment (**A**). On each frame (**B**–**F**), an automated algorithm identified the location of the two eyes (indicated by red/green dots) and the full extent of the mantle (indicated by white rectangular outline), which was cropped and rotated to align across frames (**G**–**K**). We applied principal component analysis (PCA) to the sequence of images corresponding to a square region within the mantle (indicated by blue rectangular outlines), and analyzed the time series (**M**) associated with the weight allocated to the first principal component (**L**). Example images in **G**–**K** correspond to time points indicated by blue dots in **M**.

animals (effectively treating the dataset as if it came from one aggregate animal). The analysis in **Figure 2** shows results obtained using this 'aggregate' approach. In the 'individual' analysis, PCA was applied separately to sub-stacks obtained by extracting, from the main stack, sections corresponding to individual animals. The analysis in **Figure 3** shows results obtained using this 'individual' approach. As we document in **Figure 3C** and discuss in the main text, these two analyses produced similar and internally consistent results.

Spectral profiles and distance metric

Each principal component (PC) is associated with a time series recording frame-to-frame weight allocation (see example in **Figure 1M** for the first principal component obtained by applying PCA to a small section of our dataset). We computed the power spectral density (PSD) of this series using Welch's algorithm as implemented by the scipy package (scipy.signal.welch) with default parameters (in particular, segment length is set to 256 by default), separately for each main condition (before, during, and after eating). As customary when evaluating spectral density, we logged the resulting values (see examples in **Figure 2A** for the first principal component obtained from applying PCA to the entire main stack).

To compute the spectral distance between two vectors of logged PSD values such as, for example, the vectors detailing values for two of the three traces in **Figure 2A**, we first normalized each vector to root-mean-square (RMS) equal 1, and then computed the RMS distance between the normalized vectors. We computed all three possible paired distances for the three main conditions, separately for each animal: distance between before and during, between before and after, and between during and after. To render this metric comparable across animals, we normalized the three values by dividing them by their mean for each animal. When computed across all 13 animals, this procedure generates a distance matrix of size 13×3.

To visualize the distance matrix in **Figure 2B**, we first defined a triangle for each animal with vertices labelled by main condition (before/during/after) and side lengths equal to the three distance values for that animal. We then computed its center of mass, and fixed it to the origin of the three-axis plot in **Figure 2B**. We rotated the triangle around this center to minimize the angular distance between its medians and the three axes of the plot (solid black lines oriented at 60 degrees from one another), with distance calculated between the median to the 'before' vertex and the vertical axis, between the median to the 'during' vertex and the axis down to the right, and between the median to the 'after' vertex and the axis down to the left. This procedure implements clustering of the three vertex types along the three axes, while preserving normalized distances between vertices.

Collation of manually identified T-sign samples into PC-like image

Through direct visual inspection of video footage and manual labeling, we identified a disruptive-like pattern that appeared to be preferentially expressed during non-eating phases (see drawing in **Figure 3B**). To establish a potential connection with the components returned by PCA, we averaged 30 samples of this pattern (one sample is shown in **Figure 3B**) and applied the same image processing steps described above for the main stack (conversion to monochrome, left-right symmetrization, rescaling, extraction of central square region; see orange rectangular outlines in **Figure 3B–C**).

Correlation between individual and aggregate PCs

To evaluate the correspondence between PCs from individual animals and those from the aggregate animal, we computed the pixel-by-pixel correlation between PCs. For example, the black data points in **Figure 3C** plot the correlation between the first principal component (PC1) from the aggregate animal (which is unique) and individual PC1s (x axis) or second principal components (PC2s) from different animals (each data point refers to a different animal). When computing a correlation of this kind, it is necessary to accommodate the fact that the overall sign of a given PC is arbitrary. To achieve this goal, we first computed the RMS of the difference between the two PCs to be correlated as returned by PCA, and the RMS of this difference when inverting the sign of the individual PC. If the former RMS value was smaller than the latter, we did not apply sign inversion; if otherwise, we inverted the sign of the individual PC before computing the correlation between the two PCs.

PC2/PC1 weight ratio

To evaluate the relative impact of PC2 normalized by PC1, we computed the ratio between the absolute value of PC2 weights and the absolute value of PC1 weights, then averaged this quantity over time, and logged the resulting scalar. The x axis in **Figure 3D** plots this metric averaged between before and after conditions.

Identification of footage samples potentially associated with specific PCs

PCs do not necessarily translate onto any recognizable skin pattern commonly reported in the literature, however we attempted to characterize a potential correspondence of this kind by selecting individual samples from the video recordings (see examples in **Figure 4**) based on our estimates of weight allocation to different PCs. We considered the absolute values of two time series for PC weights: a 'target' sequence, and a 'non-target' sequence. When studying PC1 (**Figure 4A–D**), the target sequence corresponded to the PC1 weight series, and the non-target sequence to the PC2 weight series. When studying PC2 (**Figure 4E–H**), we adopted the opposite attribution (target PC2, non-target PC1). For each animal separately, we selected time frames associated with target weights in the top 95th percentile. Of these selected frames, we picked the frame with smallest non-target weight, and chose the associated image sample as representative of a skin pattern that reflects the target PC (examples shown in **Figure 4**).

Statistical analysis

We performed three types of analysis in this study: test for difference from 0 (correlation values in **Figure 3C**); paired test for difference between x and y values (**Figure 3D**); comparison of spectral distance across the three main conditions (before/during/after). The first two analyses simply involved Wilcoxon tests (paired in the second case). In the third analysis, we wished to confirm the significance of the data pattern suggested by the visualization in **Figure 2B**. To achieve this goal, we first submitted the distance matrix to a Friedman test for repeated samples, which returned $p<0.01$. To determine which conditions differed and which ones did not, we then carried out a posthoc Conover Friedman Test with correction for multiple comparisons (two-stage false discovery rate), which returned no difference ($p=0.23$) between the before-during distance (separation between green and red clusters) and the during-after distance (separation between red and blue clusters), a clear difference ($p<0.01$) between the before-during distance and the before-after distance (separation between green and blue clusters), and a measurable (albeit less robust) difference between the during-after distance and the before-after distance ($p<0.05$).

RESULTS

Feeding as an experimental protocol for controlled manipulation of internal state

To study the potential impact of internal state on pattern dynamics, we must be able to produce a change in internal state over a defined period of time in a controlled manner. In other words, we must be able to produce the change reliably, and we must be able to determine when the change starts and when it ends. Furthermore, we wish to effect the change selectively without other concomitant changes, in particular we wish to minimize changes of the visual environment that may prompt camouflage. It is not easy to achieve these goals experimentally, as we further elaborate below.

The need for well-defined start and end points means that we cannot simply wait for internal states to arise spontaneously, because we do not have a meaningful protocol for defining when a given internal state arises or ends. For example, it may well be that cuttlefish experience changes in mood akin to our feelings of happiness or sadness, but we have no way of determining when those states are engaged. If we consider fear, we may induce this state by non-visual means, for example by producing a loud noise or an electric shock. These manipulations, however, would likely be associated by the animal with the presence of a physical threat such as a predator, which would prompt camouflage or, in extreme cases, hiding behavior that would make it impossible to capture pattern dynamics on video. Most other examples of internal states

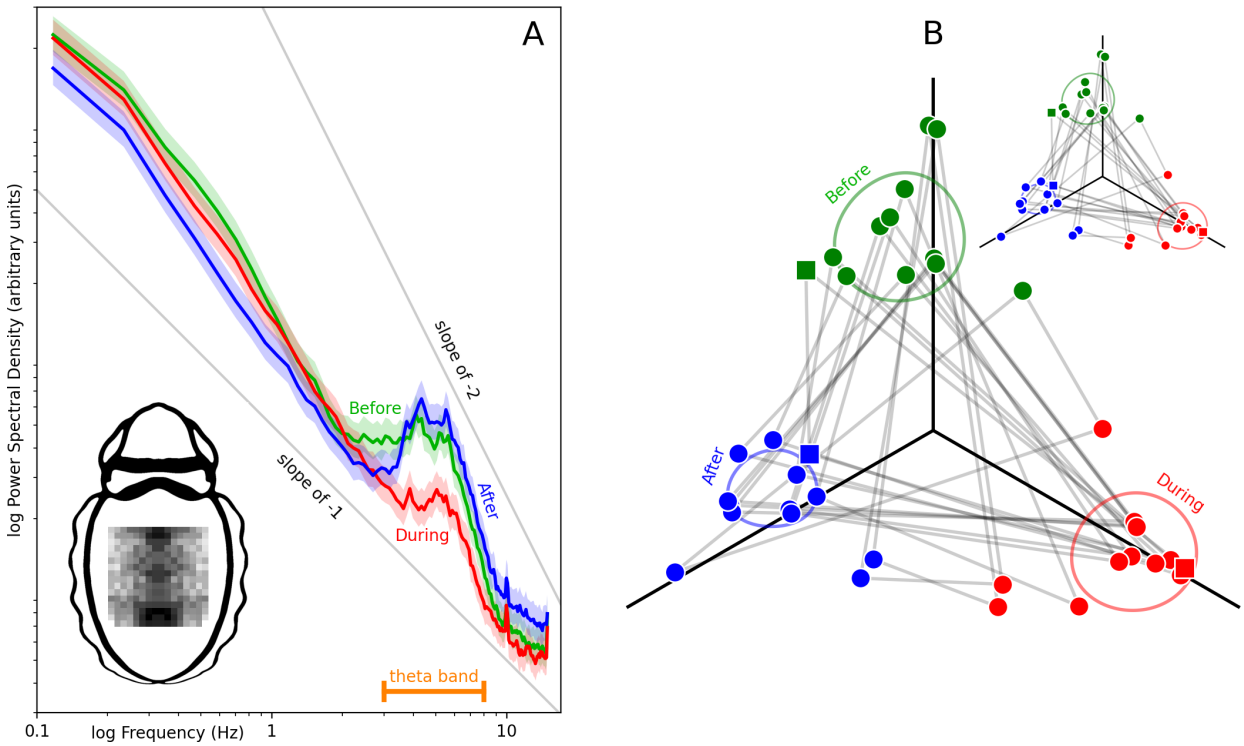

Fig. 2. Spectral density profiles for time series (such as the example in **Figure 1M**) associated with weight allocation to PC1 (shown by inset image, positioned in relation to body of cuttlefish), analyzed separately for time periods preceding (green), during (red), and following (blue) food consumption (**A**). Shaded regions indicate ± 1 SEM. The dissimilarity between two spectral profiles can be quantified via spectral distance (see Methods), indicated by the length of gray segments joining two dots in **B**. Each dot refers to a different animal engaged in one of the three feeding conditions (same color convention as in **A**). Square symbols refer to an individual who did not share the tank with any other animals. To aid visualization, dots have been positioned to retain cluster proximity with the three axes defined by black solid lines (see Methods). Oval contours reflect data spread. Inset to **B** plots equivalent results when computing PCs separately for each animal.

that may be available for experimental manipulation present similar limitations, greatly complicating the development of a selective protocol for studying this phenomenon experimentally.

Our piloting efforts towards developing a viable experimental protocol led us to focus on the act of feeding, for the following reasons. First, it is relatively easy to define when the animal starts feeding, and when it has finished feeding (see Methods for how we defined epochs). Second, if we exclude (as we did) the time period during which the prey is introduced into the tank and is visible to the cuttlefish, there is essentially no difference in the visual environment between the periods preceding/following food administration and the period associated with food consumption. Any residual difference caused by the visual appearance of the prey would also apply to the comparison between the period before feeding and the period after feeding, so the latter can be used as a control condition for this potentially confounding factor. Finally, whatever role may be ascribed to camouflage in this paradigm, it is not expected to selectively impact the feeding period: if the animal engages in cryptic behavior, we expect that this should happen during the hunting period (preceding food consumption), not during the feeding period or the period after feeding.

We recognize that, despite the above considerations, our protocol is not entirely watertight, in that it remains open to some interpretational pitfalls. At the same time, we were unable to identify a more effective paradigm for tackling our question of interest. We address potential limitations of our paradigm in the Discussion.

Principal component decomposition of skin dynamics

In this study we focus on the dynamics of large-scale patterns across the body of the cuttlefish, such as the classic 'disruptive' motif or similar macroscopic organizations of the mantle. Because these patterns must be studied with reference to the coordinate frame defined by the body of the cuttlefish, we tracked the animal over time and aligned skin patterns from different time points to form a sequence of co-registered square images, which were then subjected to conventional principal component analysis (PCA) to extract the most prominent 2D skin motifs (see Methods for details; see also Kelman et al. (2008) and Orenstein et al. (2016) for related approaches). **Figure 1L** shows the first principal component extracted from a brief period of a few minutes, alongside the change in weight associated with this component over time (**Figure 1M**). It is evident that the dynamic profile for this component is rich in structure, displaying both quick fluctuations (first 2 minutes of example in **Figure 1M**) and sustained behavior (last minute).

The most obvious tool for summarizing the dynamic range exhibited by **Figure 1M** is spectral density across temporal frequency, as shown in **Figure 2A**. This figure shows spectral density for a single component (plotted in the inset against the body of the animal) extracted from our entire dataset. Weight profiles for this component were analyzed separately for the three conditions associated with feeding: before (green), during (red), and after (blue). This analysis overlooks potential differences across animals, in

Journal of Experimental Biology (2019) 00, jebxxxxxx. doi:10.1242/jeb.xxxxxx

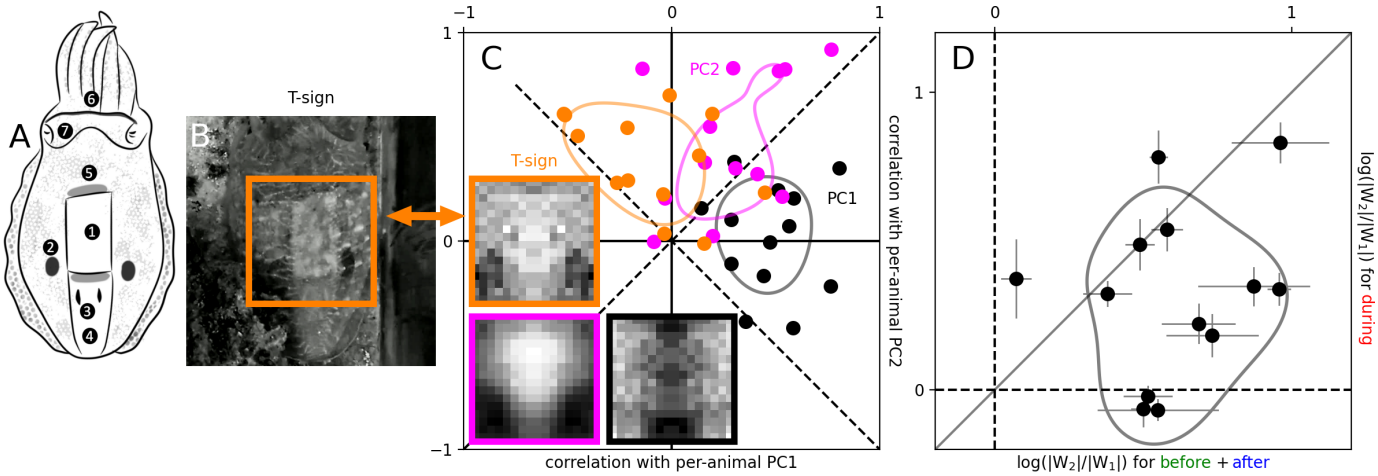

Fig. 3. Skin pattern in **A** (informally termed T-sign here) was identified via video inspection and manual labeling as being preferentially expressed during non-eating phases (see main text). We combined multiple samples of this pattern from footage (one example is shown in **B**) to obtain a component-like image (inset indicated by orange outline in **C**) comparable with those returned by PCA. **C** plots pixel-by-pixel correlation between PCA components from aggregate data (PC1/PC2 shown by insets indicated by black/magenta outlines) and equivalent PC1/PC2 components from data for individual animals on x/y axes. Black/magenta data points refer to aggregate PC1/PC2, one point per animal. Orange data points plot similar results for the T-sign pattern. **D** plots the log-ratio between absolute weight allocation to PC2 and absolute weight allocation to PC1 for individual animals (one data point per animal), averaged across time separately for non-feeding (x values) and feeding phases (y values). Error bars plot ±1 SEM in **D**. They have been omitted from **C** to avoid clutter. Numerical labels in **A** indicate white square (1), black spot (2), black bar (3), white triangle (4), black band (5), black line (6), white headband (7). Please refer to Methods for details on the procedures mentioned above.

that we are treating data from different cuttlefish as if it were collected from one 'aggregate' animal (see Methods). We confirm later in the article that our results remain consistent when taking into account individual differences.

Feeding is associated with reduced dynamics within the theta frequency range

When comparing spectral density profiles across feeding configurations, we notice a few obvious features. First, the two profiles associated with time periods outside feeding (before and after, green and blue) are very similar. More specifically, the spectral slope of the aperiodic component takes values between -1 (pink noise) and -2 (Brown noise), which is the range typically spanned by many biological signals like the electroencephalogram (EEG) (Pathania et al., 2021), and the periodic component is selectively enhanced within the theta band (Karakaş, 2020) (3–8 Hz indicated by the orange horizontal marker in **Figure 2A**), which presents increased power for both conditions. Second, the profile associated with the feeding period (red) matches the other two profiles with relation to the aperiodic component, however it presents a marked reduction of the periodic component: the power bump within the theta band is almost entirely suppressed.

Based on the qualitative observations outlined above, we devised a metric to quantify the similarity/dissimilarity between two spectral profiles (see Methods). This quantity, which we term spectral difference, can be computed for individual animals and therefore used to create a sufficiently rich dataset to support statistically informed conclusions. **Figure 2B** plots spectral difference in the form of distance across the plane: the length of a segment connecting two data points reflects the spectral difference between the two profiles associated with those points. Each point refers to one animal engaged in one feeding configuration. Overall, this plot confirms our prior observation: data clusters for the two non-feeding configurations (green/blue) are closer to each other than they are to the cluster for the feeding configuration (red). This pattern is statistically significant (see Methods).

Inter-individual consistency of extracted components

The analysis in **Figure 2B** separates time series of component weights by feeding condition and tested animal, however the weights are computed for one principal component (shown by the inset to **Figure 2A**) obtained across the entire dataset. When we repeat this analysis by separately extracting components from data for individual animals, the outcome is very similar to that obtained in **Figure 2B**, as plotted in the inset to that figure. From this plot, however, it is not possible to infer whether the principal component from animal A, for example, looks like the principal component from animal B. The similarity between the two outcomes (compare main panel with inset in **Figure 2B**) suggests that components extracted separately from different animals should be largely similar, however we wished to confirm this expectation with direct analysis.

Figure 3C quantifies the pixel-by-pixel correlation between principal components extracted from the entire dataset and equivalent components extracted from individual animals. More specifically, x values plot correlations with the first principal component (PC1) from individual cuttlefish (one data point per animal), while y values plot correlations with individual second principal components (PC2). The aggregate PC1 obtained from the entire dataset (inset image indicated by black outline, same as inset to **Figure 2A**) correlates with PC1 estimates from individual animals (black data points fall to the right of vertical solid line at $p < 0.001$, indicating positive correlation), but does not correlate with individual PC2 estimates (black data points scatter around horizontal solid line at $p=0.94$). The aggregate PC2 (inset image indicated by magenta outline) correlates substantially with individual PC2 estimates (average coefficient of 0.48, magenta data points fall above horizontal solid line at $p < 0.001$). It also correlates, to a lesser extent (average coefficient of 0.28), with individual PC1 estimates (magenta data points fall to the right of vertical solid line at $p < 0.01$), indicating weaker correspondence between aggregate and invidual estimates for PC2. Overall, this pattern of results

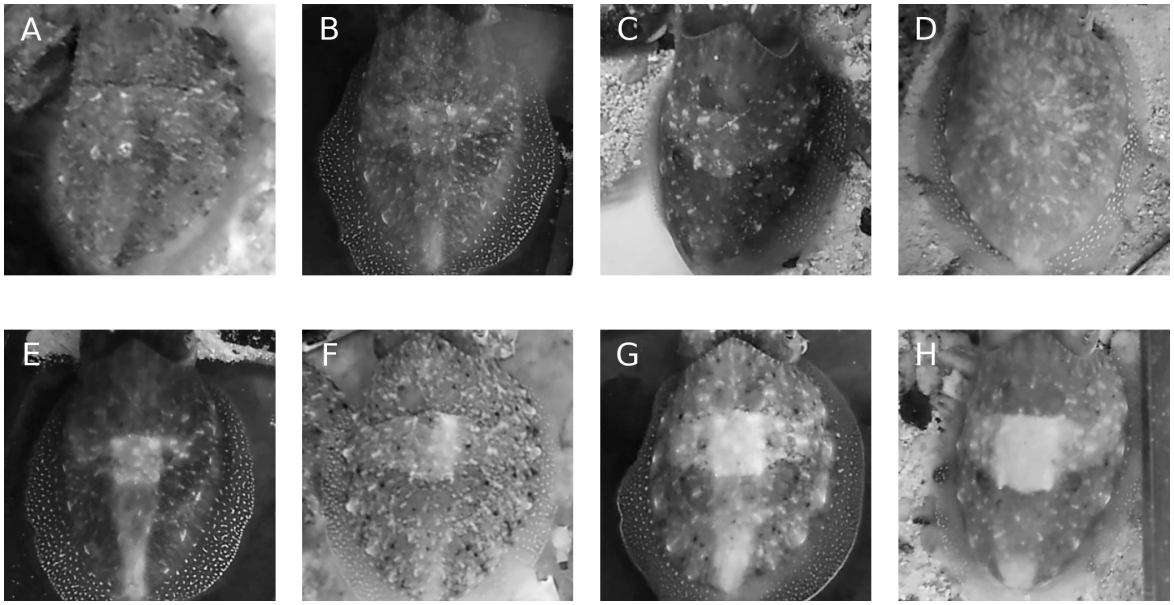

Fig. 4. Skin patterns tentatively corresponding to PC1 (**A**–**D**) and PC2 (**E**–**H**), automatically selected by an algorithm that relies on PC weight allocation (see Methods).

is indicative of consistent structure between PC estimates from the aggregate dataset and corresponding estimates from individual animals, with some residual misalignment for PC2.

Enhanced relative expression of second component during non-feeding epochs

In the early stages of this project, we attempted manual labelling of pattern expression for a subset of our database. These pilot measurements identified a specific pattern (which we term T-sign) as being over-expressed before and after feeding (see drawing in **Figure 3A** and sample from footage in **Figure 3B**). This pattern, which we have extracted from hand-picked images and formatted to align with our PCA estimates (inset image indicated by orange outline in **Figure 3C**), appeared with the following frequencies averaged across four animals: 40% (before), 4% (during), and 56% (after). To investigate this effect using automated methods, we first established whether the T-sign pattern presented some connection with our estimated PCs. As indicated by the orange data points in **Figure 3C**, which plot pixel-by-pixel correlations between the T-sign and individual PC1/PC2 estimates (same convention adopted for aggregate PCs), this pattern presents substantial similarity with PC2 (orange data points fall above horizontal solid line at $p < 0.001$, but scatter around vertical solid line at $p=0.17$).

Guided by the above analysis, we proceeded to estimate the log-ratio between absolute weights for PC2 versus PC1 (see Methods), separately for the feeding condition (y axis in **Figure 3D**) and for the non-feeding conditions (x axis). The results of this additional analysis provide tentative support for our earlier informal observations from manual labeling: data points tend to fall below the unity line in **Figure 3D**, indicating over-expression of PC2 (compared with PC1) during the non-feeding epochs ($p<0.02$ for direct comparison between y and x values using a paired Wilcoxon test).

Tentative connection between specific components and known skin patterns

The components extracted by PCA are not necessarily interpretable with relation to specific skin patterns commonly observed in cuttlefish, because they represent statistical constructs that capture the contribution of elements that may appear in multiple patterns and often in combination with other components that may distort their visual appearance. With this caveat in mind, it is nevertheless helpful to establish at least a tentative link with well-known patterns, such as mottle or disruptive. To make a first step in this direction, we applied a selection procedure to individual frames from the original footage that made it possible to identify individual images potentially representative of skin patterns that are more directly relevant to specific PCs than others (see Methods). For example, **Figure 4A**–**D** show samples from four different animals that are connected with large weight on PC1 and small weight on PC2, while **Figure 4E**–**H** show samples for the opposite PC weight allocation (large on PC2, small on PC1).

The examples in **Figure 4** inevitably present some differences, however they also share some features that allow for a qualitative interpretation of how PC1 and PC2 may correspond, at least coarsely, to specific skin patterns that have been reported in prior literature. More specifically, PC1 appears to associate with the four-dot pattern marking the vertices of the central square, while PC2 presents scattered connections with the disruptive display, although often in combination with a vertical bright bar running across the body (**Figure 4E**,**G**). The pattern for PC2, in fact, resembles the pattern identified via manual labeling (**Figure 3B**), consistent with the analysis reported in **Figure 3C**–**D**.

We must caution readers against reading too much into **Figure 4**. First, our methodology for identifying the examples in that figure did not always return consistent results across all animals. Second, individual images always present inevitable registration misalignments with respect to other images, which can lead to artefactual conclusions when visually extrapolating features from single frames to the whole dataset. While it is important to see original images to establish a connection with known footage in cuttlefish, these images are not and cannot be representative of the ensemble analysis effected by PCA. Third, as pointed out above, PCs are not transparently connected with full skin displays typically seen in cuttlefish. Finally, it is virtually impossible to

completely separate different PCs at the level of individual images, meaning that a given image reflects multiple contributions from different PCs, greatly reducing its interpretability.

For the above reasons, we view **Figure 4** as a suboptimal qualitative tool for mapping known concepts onto our results, with the understanding that any specific inference about the role of known patterns, such as disruptive or others, is not entirely warranted, and that future studies will be necessary to fully elucidate the potential role of those patterns in expressing internal states. As a consequence, in the remaining part of the article we do not further discuss the results in **Figure 4**, but rather leave them as open suggestions for future research.

DISCUSSION

Our primary observation is that the internal state experienced by the animal when feeding is associated with specific changes in the expression and dynamics of mantle patterns. More specifically, we found that theta fluctuations of the first principal component extracted from a square region of the mantle is engaged primarily during non-feeding behavior, being almost entirely suppressed during feeding behavior. We also found that the second principal component is expressed more often during non-feeding behavior, although the extraction of this result from data was guided by non-automated inspection of the dataset, which reduces its reliability and calls for further confirmation by future studies. Below we discuss relevant connections with existing literature, unaddressed interpretational difficulties, and potential implications for our broader understanding of spontaneous pattern dynamics in cephalopods.

Relations to existing literature

We are not aware of any prior studies that specifically investigated pattern dynamics during feeding in cuttlefish. The only published study that indirectly touched on this issue involved recording body patterns while animals were engaged in a range of behavioral contexts, with food consumption being one of the labelled behaviors (Crook et al., 2002). However, this prior study did not examine potential differences in body pattern expression/dynamics for different behaviors or, if the authors did examine such potential differences, they did not report on the results of their investigation, choosing instead to focus on pattern characteristics that presumably generalized across behaviors. In a different study on sleep in cuttlefish (Iglesias et al., 2019), the authors cursorily mention that 'animals primarily maintained some variation of the mottle pattern (Chiao et al., 2010) unless feeding or disturbed by human activity,' which suggests that these authors anecdotally observed pattern changes during feeding. Unfortunately, they do not provide any further information with regard to this observation, as it did not represent the focus of their study.

A few prior studies examined behavioral patterns associated with feeding in octopus. Some species, like the larger pacific striped octopus, acquire specific postures while feeding, and frequently express certain high-contrast patterns when observing a conspecific engaged in feeding behavior (Caldwell et al., 2015). Other species have been recorded in the wild to express identifiable patterns more frequently when feeding (Mather and Mather, 1994), although the degree of specificity associated with this phenomenon was relatively weak.

In general, food consumption *per se* (as a separate act that does not include hunting or prey capture) is largely neglected by studies of pattern dynamics in cephalopods, with most studies focusing on other behaviors, such as foraging or mating. The most plausible explanation for this lack of interest in the act of feeding is that this behavior is not expected to involve either camouflage or communication, and is therefore regarded as an unlikely source of complex pattern dynamics. It is for those same reasons, however, that we focused on feeding in this study, as it potentially offers the opportunity to study skin dynamics during undirected behavior.

Potential confounds and artefacts

As anticipated in the Results section when motivating our focus on feeding behavior, any experimental attempt at manipulating the internal state of an animal is saddled with serious interpretational difficulties, which also inevitably apply to our own protocol. Below we discuss what we consider to be the most significant limitations of our experimental design.

Our protocol is predicated on the notion that neither camouflage nor communication are selectively engaged during food consumption. By 'selectively' we mean that, if these processes are engaged at all, they are equally engaged before, during, and after feeding. Cuttlefish were filmed without removing them from the tank in which they lived, and the tank contained various natural features, such as rocks and plants. They were never exposed to predators (or any other threat), so there is no reason to expect that they would attempt to camouflage in order to escape predation. It is possible that they engaged in camouflage (or other forms of pattern expression related to foraging) while hunting shrimps, however these time periods were removed from our analysis (see Methods). It should also be noted that, because the environment was stable, the component resembling its structure (presumably the first component) would also be similar across epochs and, furthermore, it should be over-expressed during camouflage. This is not, however, what we observed: although the *dynamics* (spectral profile) of the first component differed during food consumption, its overall expression (weight variance) was virtually identical across phases. In other words, although skin pattern dynamics differed between feeding and non-feeding phases, skin pattern expression was overall equally rich across phases, inconsistent with a straightforward explanation based on camouflage.

With regard to communication with conspecifics occupying the same tank, it is unclear why this behavior should be selectively engaged (or not) during feeding. Furthermore, the best individual example of the data pattern shown in **Figure 2B** comes from a cuttlefish named Giulia, who never shared her tank with any other animal. Results for this individual are highlighted by square symbols in **Figure 2B**. These measurements are more reliable than those obtained from all other individuals, because we were able to carry out more experiments with this animal thanks to its longevity. Based on these and the above considerations, we conclude that camouflage and communication are unlikely to play a counfounding role in our experiments. At the same time, we recognize that we cannot completely exclude the possibility that, during food consumption, cuttlefish may engage in behavior that is somehow connected with agents/factors beyond their own internal state. Our position is that, all elements considered, there is no compelling reason to hypothesize selective involvement of camouflage/communication while feeding.

A different class of interpretational difficulties arises in connection with metabolic state. During food consumption, cuttlefish

must engage metabolic processes associated with digestive functions, which may in turn alter the allocation of energy resources to other organs, such as the mantle display. These internal changes may instantiate a state akin to sleep, which has been reported to associate with specific skin displays in cephalopods, such as the 'half-and-half' pattern in octopus (Meisel et al., 2011) and the 'dark arms' component or mottle variants in cuttlefish (Iglesias et al., 2019; Frank et al., 2012). We think this interpretation is unlikely, because feeding is an active behavior that is not normally associated with sleeping in cuttlefish, however it is possible that these two states share some characteristics. More generally, it is difficult to speculate on which specific internal characteristics of the feeding process may be reflected by changes in skin pattern dynamics. Based on the nature of our experimental design and associated measurements, we can reasonably characterize our results as primarily pertaining to a state that is internal to the animal and is largely decoupled from environmental specifics and/or interaction with other animals. Any inference beyond this statement, which we tentatively address below, remains highly speculative.

Tentative interpretation with reference to reward-based behavior

Previous research has demonstrated that the administration of unexpected food rewards to cuttlefish can modify their subsequent behavior (Chung et al., 2022). More specifically, the results of these experiments have been interpreted to indicate that changes in the internal state of the animal, such as 'liking' the food or 'wanting' more of it, may shape their foraging strategy in response to additional food items. We favour an interpretation along similar lines for our own results, namely we hypothesize that the feeding-specific changes in pattern dynamics exposed by our measurements reflect a positive reaction to food consumption, which may in turn be associated with the release of specific neurotransmitters such as dopamine (Heymann et al., 2020) and/or serotonin (Palovcik et al., 1982). Under this interpretation, the effects we report here would not be specific to food, but would generalize to other forms of reward, including those potentially associated with mating and socialization. In those contexts, it may be more difficult to experimentally isolate skin pattern components that are specific to reward-driven internal states as opposed to outward-directed communication signals, however similar mechanisms may be at play.

Following on from the above hypothesis, it is tempting to draw a parallel between our finding of theta-specific dynamic changes in pattern expression (**Figure 2A**) and the established role of theta oscillations in reward-based learning across vertebrates (Zold and Hussain Shuler, 2015; van Wingerden et al., 2010; Knudsen and Wallis, 2020), including humans (Lin et al., 2022). A parallel of this kind, however, is problematic in view of several considerations. First, theta oscillations in neuronal activity, such as those that may be measured via local field potentials or EEG (Karakaş, 2020), are completely different from oscillations in skin pattern dynamics. It is possible that the two phenomena are connected: it is known, for example, that specific pattern dynamics are likely controlled by central pattern generators (Laan et al., 2014), and those same generators may also drive EEG signals (Berkowitz, 2019). There is no evidence, however, to suggest that one may directly compare frequency bands between brain activity and skin dynamics. Even if one were to accept a comparison of this kind, it would involve wildly different animals: most evidence on the role of theta oscillations in reward-based and memory-based behavior comes from vertebrates (Karakaş, 2020). The specifics of our dataset bring additional difficulties to a theta-based interpretation. For example, spectral profiles vary substantially across animals. These inter-individual differences are incorporated into our distance metric (**Figure 2B**), however they are not adequately captured by the aggregate plot in **Figure 2A**. As a consequence, the theta-specific effect exposed by the aggregate plot may only represent a partial view of the entire phenomenon, which is likely far more complex and individually idiosyncratic. Finally, even if we were to overlook all the complications listed above, based on prior literature we expect an increase, not a decrease, of theta power during feeding, which is opposite to what we observe. For all these reasons, although we cannot exclude that the theta specificify of our results may reflect a deeper connection with neuronal oscillations in central areas, we regard this hypothesis as entirely speculative at this stage.

Implications for understanding internal states in invertebrates

We conclude by considering the more general question of whether it is plausible to hypothesize that cuttlefish may express their internal state via overt mantle displays, and what the implications may be for a wider understanding of invertebrate cognition. It is currently undisputed that invertebrate behavior is conditional upon internal states (Brembs, 2013): to mention just a couple of relevant results, the satiation state of the predatory sea-slug *Pleurobranchea* regulates approach/avoidance behavior in this animal (Hirayama and Gillette, 2012), and feeding state impacts navigational choices in both bees (Dyer et al., 2002) and ants (Harris et al., 2005).

It remains unclear, however, whether internal states may also be expressed by skin pattern changes (in animals that are capable of producing them) that are not outward-directed in the immediate sense, that is to say not directed towards the environment (camouflage) or other animals (communication). In some lizard species, for example, exposure to stressful conditions can dynamically modify body coloration (Boyer and Swierk, 2017; Greenberg, 2002), and related effects have been reported in some amphibians (Kindermann et al., 2013). In all these cases, as in ours, it is difficult to be certain that the observed changes do not reflect some form of communication/camouflage, if not actualized at least intended. Notwithstanding these interpretational difficulties, based on our results we propose that the possibility of implicit (non-communicative) displays of internal states in invertebrates should be entertained by future studies. The implications brought about by this possibility are wide-ranging. We do not envisage that they should extend to controversial and complex phenomena like sentience (Mather, 2022), but rather we maintain that, from a purely behavioral standpoint, the existence of such phenomena would provide experimentalists with novel ways to access the cognition of creatures that are evolutionarily distant from us, yet possibly share some primordial internal states with our own species.

Funding

Supported by L'Oréal (Chaire Beauté(s)), CNRS, ANR-10-LABX-0087 IEC, and ANR-10-IDEX-0001-02 PSL*.

Supplementary

Supplementary Video Example of tracking/alignment for a short video-recording of spontaneous behavior in one participant. Color video (left) shows original footage, grayscale video (right) shows tracked/aligned animal.

REFERENCES

A. Barbosa, L. M. Mäthger, K. C. Buresch, J. Kelly, C. Chubb, C. C. Chiao, and R. T. Hanlon. Cuttlefish camouflage: the effects of substrate contrast and size in evoking uniform, mottle or disruptive body patterns. *Vision Res*, 48 (10):1242–1253, May 2008.

A. Berkowitz. Expanding our horizons: central pattern generation in the context of complex activity sequences. *J Exp Biol*, 222(Pt 20), Oct 2019.

Jane F.F. Boyer and Lindsey Swierk. Rapid body color brightening is associated with exposure to a stressor in an anolis lizard. *Canadian Journal of Zoology*, 95(3):213–219, 2017.

B. Brembs. Invertebrate behavior—actions or responses? *Frontiers in Neuroscience*, 7, 2013. doi: 10.3389/fnins.2013.00221.

R. L. Caldwell, R. Ross, A. Rodaniche, and C. L. Huffard. Behavior and Body Patterns of the Larger Pacific Striped Octopus. *PLoS One*, 10(8):e0134152, 2015.

C. C. Chiao, C. Chubb, K. C. Buresch, A. Barbosa, J. J. Allen, L. M. Mäthger, and R. T. Hanlon. Mottle camouflage patterns in cuttlefish: quantitative characterization and visual background stimuli that evoke them. *J Exp Biol*, 213 (2):187–199, Jan 2010.

T. T. Chung, A. S. Darmaillacq, L. Dickel, and C. C. Chiao. The effect of unexpected rewards on decision making in cuttlefish. *Sci Rep*, 12(1):2514, Feb 2022.

A. C. Crook, R. Baddeley, and D. Osorio. Identifying the structure in cuttlefish visual signals. *Philos Trans R Soc Lond B Biol Sci*, 357(1427):1617–1624, Nov 2002.

F. C. Dyer, M. Gill, and J. Sharbowski. Motivation and vector navigation in honey bees. *Naturwissenschaften*, 89(6):262–264, Jun 2002.

A. El Nagar, D. Osorio, S. Zylinski, and S. M. Sait. Visual perception and camouflage response to 3D backgrounds and cast shadows in the European cuttlefish, Sepia officinalis. *J Exp Biol*, 224(11), Jun 2021.

R. C. Feord, M. E. Sumner, S. Pusdekar, L. Kalra, P. T. Gonzalez-Bellido, and T. J. Wardill. Cuttlefish use stereopsis to strike at prey. *Sci Adv*, 6(2): eaay6036, Jan 2020.

G. Fiorito, A. Affuso, J. Basil, A. Cole, P. de Girolamo, L. D'Angelo, L. Dickel, C. Gestal, F. Grasso, M. Kuba, F. Mark, D. Melillo, D. Osorio, K. Perkins, G. Ponte, N. Shashar, D. Smith, J. Smith, and P. L. Andrews. Guidelines for the Care and Welfare of Cephalopods in Research -A consensus based on an initiative by CephRes, FELASA and the Boyd Group. *Lab Anim*, 49(2 Suppl):1–90, Jul 2015.

M. G. Frank, R. H. Waldrop, M. Dumoulin, S. Aton, and J. G. Boal. A preliminary analysis of sleep-like states in the cuttlefish Sepia officinalis. *PLoS One*, 7(6):e38125, 2012.

A. Galán, W.-S. Chung, and N. Marshall. Dynamic courtship signals and mate preferences in sepia plangon. *Frontiers in Physiology*, 11, 08 2020. doi: 10.3389/fphys.2020.00845.

N. Greenberg. Ethological Aspects of Stress in a Model Lizard, Anolis carolinensis. *Integr Comp Biol*, 42(3):526–540, Jul 2002.

R. T. Hanlon and J. B. Messenger. *Cephalopod Behaviour*. Cambridge: Cambridge University Press, 1996.

R. A. Harris, N. Hempel de Ibarra, P. Graham, and T. S. Collett. Ant navigation: priming of visual route memories. *Nature*, 438(7066):302, Nov 2005.

Kaiming He, Georgia Gkioxari, Piotr Dollar, and Ross Girshick. Mask r-cnn. In *Proceedings of the IEEE International Conference on Computer Vision (ICCV)*, pages 2961–2969, Oct 2017.

G. Heymann, Y. S. Jo, K. L. Reichard, N. McFarland, C. Chavkin, R. D. Palmiter, M. E. Soden, and L. S. Zweifel. Synergy of Distinct Dopamine Projection Populations in Behavioral Reinforcement. *Neuron*, 105(5):909–920, Mar 2020.

K. Hirayama and R. Gillette. A neuronal network switch for approach/avoidance toggled by appetitive state. *Curr Biol*, 22(2):118–123, Jan 2012.

M. J. How, M. D. Norman, J. Finn, W. S. Chung, and N. J. Marshall. Dynamic Skin Patterns in Cephalopods. *Front Physiol*, 8:393, 2017.

Teresa L. Iglesias, Jean G. Boal, Marcos G. Frank, Jochen Zeil, and Roger T. Hanlon. Cyclic nature of the REM sleep-like state in the cuttlefish Sepia officinalis. *Journal of Experimental Biology*, 222(1), 01 2019. ISSN 0022-0949. doi: 10.1242/jeb.174862. URL https://doi.org/10.1242/jeb.174862.jeb174862.

Sirel Karakaş. A review of theta oscillation and its functional correlates. *International Journal of Psychophysiology*, 157:82–99, 2020. ISSN 0167-8760. doi: https://doi.org/10.1016/j.ijpsycho.2020.04.008. URL https://www.sciencedirect.com/science/article/pii/S0167876020300763.

E. J. Kelman, D. Osorio, and R. J. Baddeley. A review of cuttlefish camouflage and object recognition and evidence for depth perception. *J Exp Biol*, 211(Pt 11):1757–1763, Jun 2008.

C. Kindermann, E. J. Narayan, F. Wild, C. H. Wild, and J. M. Hero. The effect of stress and stress hormones on dynamic colour-change in a sexually dichromatic Australian frog. *Comp Biochem Physiol A Mol Integr Physiol*, 165(2): 223–227, Jun 2013.

E. B. Knudsen and J. D. Wallis. Closed-Loop Theta Stimulation in the Orbitofrontal Cortex Prevents Reward-Based Learning. *Neuron*, 106(3): 537–547, May 2020.

A. Laan, T. Gutnick, M. J. Kuba, and G. Laurent. Behavioral analysis of cuttlefish traveling waves and its implications for neural control. *Curr Biol*, 24 (15):1737–1742, Aug 2014.

K. V. Langridge, M. Broom, and D. Osorio. Selective signalling by cuttlefish to predators. *Curr Biol*, 17(24):R1044–1045, Dec 2007.

M. H. Lin, O. Liran, N. Bauer, and T. E. Baker. Scalp recorded theta activity is modulated by reward, direction, and speed during virtual navigation in freely moving humans. *Sci Rep*, 12(1):2041, Feb 2022.

J. A. Mather and L. Mather. Skin colours and patterns of juvenile *Octopus vulgaris* (Mollusca, Cephalopoda) in Bermuda. *Vie et Milieu / Life & Environment*, 44(3/4):267–272, 1994.

Jennifer Mather. The case for octopus consciousness: Valence. *NeuroSci*, 3 (4):656–666, 2022. ISSN 2673-4087. doi: 10.3390/neurosci3040047. URL https://www.mdpi.com/2673-4087/3/4/47.

D.V. Meisel, R.A. Byrne, J. A. Mather, and M. Kuba. Behavioral sleep in Octopus Vulgaris. *Vie et milieu - Life and Environment*, 61(4):185–190, 2011.

K. Okamoto, H. Yasumuro, A. Mori, and Y. Ikeda. Unique arm-flapping behavior of the pharaoh cuttlefish, *Sepia pharaonis*: putative mimicry of a hermit crab. *J Ethol*, 35(3):307–311, 2017.

Eric C. Orenstein, Justin M. Haag, Yakir L. Gagnon, and Jules S. Jaffe. Automated classification of camouflaging cuttlefish. *Methods in Oceanography*, 15-16:21–34, 2016. ISSN 2211-1220. doi: https://doi.org/10.1016/j.mio.2016.04.005. URL https://www.sciencedirect.com/science/article/pii/S2211122015300220. Computer Vision in Oceanography.

D. Osorio, F. Nager, C. W. Tyler, and A. S. Darmaillacq. Multi-level control of adaptive camouflage by European cuttlefish. *Curr Biol*, 32(11):2556–2562, Jun 2022.

R. A. Palovcik, B. A. Basberg, and J. L. Ram. Behavioral state changes induced in Pleurobranchaea and Aplysia by serotonin. *Behav Neural Biol*, 35(4):383–394, Aug 1982.

A. Pathania, M. Schreiber, M. W. Miller, M. J. Euler, and K. R. Lohse. Exploring the reliability and sensitivity of the EEG power spectrum as a biomarker. *Int J Psychophysiol*, 160:18–27, Feb 2021.

Sam Reiter and Gilles Laurent. Visual perception and cuttlefish camouflage. *Current Opinion in Neurobiology*, 60:47–54, 2020. ISSN 0959-4388. doi: https://doi.org/10.1016/j.conb.2019.10.010. URL https://www.sciencedirect.com/science/article/pii/S0959438819301187. Neurobiology of Behavior.

M. van Wingerden, M. Vinck, J. Lankelma, and C. M. Pennartz. Theta-band phase locking of orbitofrontal neurons during reward expectancy. *J Neurosci*, 30(20):7078–7087, May 2010.

C. L. Zold and M. G. Hussain Shuler. Theta Oscillations in Visual Cortex Emerge with Experience to Convey Expected Reward Time and Experienced Reward Rate. *J Neurosci*, 35(26):9603–9614, Jul 2015.

S. Zylinski, D. Osorio, and A. J. Shohet. Cuttlefish camouflage: context-dependent body pattern use during motion. *Proc Biol Sci*, 276(1675): 3963–3969, Nov 2009.